Inorg. Chem. **2007**, *46*, 10632–10638

Fine-Tuning Ligand–Receptor Design for Selective Molecular Recognition of Dicarboxylic Acids

Arnau Arbuse,[†] Carmen Anda,[†] Ma Angeles Martínez,*[,†] Javier Pérez-Mirón,[‡] Carlos Jaime,[‡] Teodor Parella,[§] and Antoni Llobet*[,||]

Departament de Química, Universitat de Girona, Campus de Montilivi, E-17071 Girona, Spain, Servei de RMN and Departament de Química, Universitat Autònoma de Barcelona, Cerdanyola del Vallès, E-08193 Barcelona, Spain, and Institute of Chemical Research of Catalonia (ICIQ), Av. Països Catalans 16, E-43007 Tarragona, Spain

Received June 29, 2007

The host–guest interaction between the hexaaza macrocyclic ligand 3,7,11,18,22,26-hexaazatricyclo[26.2.2.2^{13,16}]-tetratriaconta-1(31),13(34),14,16(33),28(32),29-hexaene (*P*3) and three rigid dicarboxylic acids (isophthalic acid, H_2*is*; phthtalic acid, H_2*ph*; and terephthalic acid, H_2*te*) has been investigated using potentiometric equilibrium methods and NMR spectroscopy including the measurement of intermolecular nuclear Overhauser effects (NOEs) and self-diffusion coefficients (*D*). Ternary complexes are formed in aqueous solution as a result of hydrogen bond formation and Coulombic interactions between the host and the guest. In the $[(H_6P3)(is)]^{4+}$ complex, those bonding interactions reach a maximum yielding a log K_6^R of 4.74. Competitive distribution diagrams and total species distribution diagrams are used to illustrate the main features of these systems. In particular, a selectivity of over 89% at p[H] = 5.0 is obtained for the complexation of the *is* versus the *te* substrates. The recognition capacity of *P*3 over dicarboxylic acids (*da*) is compared to the related hexaaza macrocycle Me_2P3 (7,22-dimethyl-3,7,11,18,22,26-hexaazatricyclo-[26.2.2.2^{13,16}]tetratriaconta-1(30),13,15,28,31,33-hexaene) that binds *da* with a lesser strength, and it is not selective. Theoretical calculations performed at molecular dynamics level have also been carried out and point out that the origin of selectivity is mainly due to the capacity of the *P*3 ligand receptor to adapt to the geometry of the dicarboxylic acid to form relatively strong hydrogen bonds.

Introduction

The design of host molecules as receptors for the recognition of substrate anion guest molecules in aqueous solution is an important target from an environmental, industrial, and health-related point of view with multiple potential applications.[1] Recently, Bowman-James, through a systematic investigation of the influence of dimensionality, hydrogen bonding, topology, and charge complementarities, has established the foundation for understanding the roles that these aspects play in anion binding and selectivity. Bowman-James has categorized the binding of anions in terms of their coordination numbers and geometries similar to transition-metal coordination on the basis of Werner's predictions.[2]

In this context, the synthetic versatility of polyamine macrocyclic receptors containing appropriate binding sites and cavities of suitable size and shape have been widely used as anion binding hosts.[2−4] On the other hand, dicarboxylate ion recognition is of great biological and medicinal relevance, as many dicarboxylates take part in metabolic process and

* To whom correspondence should be addressed. E-mail: allobet@ici.es.
[†] Universitat de Girona.
[‡] Departament de Química, Universitat Autònoma de Barcelona.
[§] Servei de RMN, Universitat Autònoma de Barcelona.
[||] Institute of Chemical Research of Catalonia (ICIQ) and Departament de Química, Universitat Autònoma de Barcelona.

(1) (a) Lehn, J.-M. *Supramolecular Chemistry;* VCH: New York, 1995. (b) Martell, A. E. *Oxigen Complexes and Oxigen Activacion by Transition Metals*; Plenum: New York, 1988. (c) Zang, V.; van Eldik, R. *Inorg. Chem*. **1990**, 29, 4463. (d) Franz, K. J.; Lippard, S. J. *J. Am. Chem. Soc.* **1999**, *121*, 10594. (e) Hosseini, M. W.; Lehn, J.-M.; Mertes, M. P. *Helv. Chim. Acta* **1983**, *66*, 2454. (f) Bencini, A.; Bianchi, A.; Scott, E. C.; Morales, M.; Wang, B.; Garcia-España, E.; Deffo, T.; Takusagawa, F.; Mertes, M. P.; Mertes, K.-B.; Paoletti, P. *Bioorg. Chem*. **1992**, *20*, 8. (g) Izatt, R. M.; Pawlak, K.; Bruening, R. L. *Chem. Rev.* **1995**, *95*, 2529. (h) Formica, M.; Fusi, V.; Micheloni, M.; Pontellini, R.; Romani, P. *Coord. Chem. Rew.* **1999**, *184*, 347−363. (i) Sun, X.; Wuest, M.; Weisman, G. R.; Wong, E. H.; Reed, D. P.; Boswell, C. A.; Motekaitis, R.; Martell, A. E.; Welch, M. J.; Anderson, C. J. *J. Med. Chem.* **2002**, *45*, 469−477. (j) Anda, C.; Martinez, M. A.; LLobet, A. *Supramol. Chem.* **2005**, *17* (*3*), 257−266.

10.1021/ic701288n CCC: $37.00
Published on Web 11/08/2007

energy storage.[5] Enzymes, antibodies, amino acids, and metabolic intermediates, as well as other natural products, contain a range of carboxylate functionalities that, in some instances, account for the characteristic biochemical behavior.[4,6]

Within this field, we have undertaken a systematic evaluation of molecular recognition phenomena between different dicarboxylic acids on the basis of a family of ditopic hexaazamacrocyclic ligands containing *meta*- and *para*-xylylic spacers and different content of methylenic units within amine groups.[6c] In this Work, we have shown how the appropriate hexaazamacrocyclic ligand, under the right conditions, can strongly and selectively bind to oxalate, a rigid substrate, and generate weaker interactions with other flexible dicarboxylic acids like oxidiacetic acid.

We are now focusing our attention to the molecular recognition of benzenedicarboxylic acid isomers. These dicarboxylates can be considered as ideal models for rigid anionic substrates having well-defined shapes in terms of charge density and hydrogen bonding.[4] In the present Work, we report the recognition capacity of ditopic hexaazamacrocycle ligands on the basis of *p*-xylyl spacers with regard to isophthalic acid (H_2*is*), phthtalic acid (H_2*ph*), and terephthalic acid (H_2*te*) and compare it with a recently reported Me_2*P*3 analogue[7] (see Chart 1).

Experimental Section

Materials. NMe_4Cl (purum >98%), phthalic acid (ACS reagent >99.5%), isophthalic acid (purum, 99%), and terephthalic acid disodium salt (purum 96%) were commercial products obtained from Aldrich and were used without further purification. Hydrochloric acid solution 0.1 mol/L and tetramethylammonium hydroxide solution 10% were purchased from Merck. The degasified solution of tetramethylammonium hydroxide was standarized with potassium hydrogen phthalate. Ligand *P*3 was prepared as a colorless hexabromide salt (*P*3.6HBr) according to previously published procedures[8] (see Chart 1 for abbreviation used).

Chart 1. Drawings and Abbreviations for the Ligands and Substrates

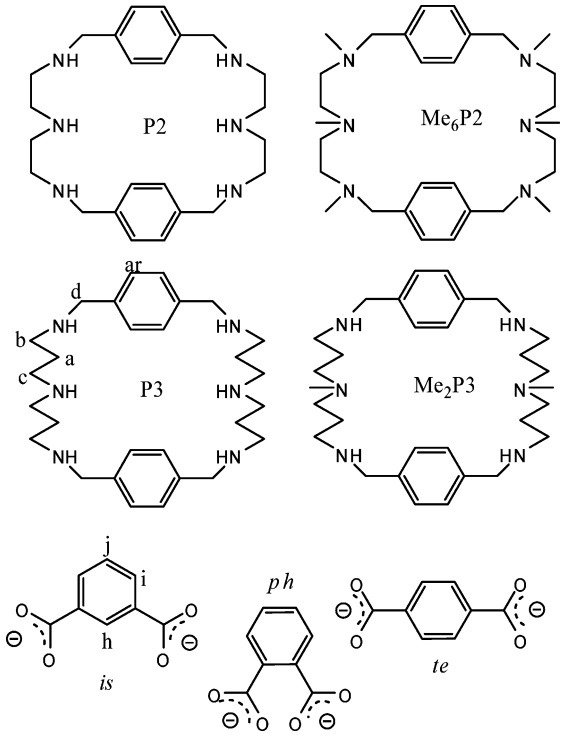

Potentiometric Titrations. Potentiometric measurements were conducted in a jacketed cell thermostated at 25.0 °C and were kept under an inert atmosphere of purified and humidified argon. For the potentiometric measurements, a Crison pHmeter (Model 2002) was used equipped with a glass electrode and a Ag/AgCl reference electrode with saturated KCl as internal solution. The volume of titrating agent to be added to the reaction mixture was controlled by means of an electronic Crison burette with a nominal volume of 1 mL. The support electrolyte used to keep ionic strength constant at 0.10 M was NMe_4Cl. The combined glass electrode (Metrohm 6.0255.100) was calibrated as a hydrogen concentration probe by titrating known amounts of HCl with CO_2-free NMe_4OH solutions and by determining the equivalent point by Gran's method[9] that allows to calculate the standard potential (E^0) and the ionic product of water (pK_w). Log K_w for the system, defined in terms of $\log([H^+][OH^-])$, was found to be −13.83 at 298.1 K in 0.1mol/L NMe_4Cl and was kept fixed during refinements.

Acid dissociation constants for the phthalic and isophthalic acids were determined under exact conditions employed in this work and were found to agree well with data from the literature.[10] Because of its insolubility on the medium used, acid dissociation constants for the terephthalic acid were obtained from the literature.[11]

Potentiometric measurements of solutions either containing the ligand or the ligand plus equimolecular amounts of phthalic acid, isophthalic acid, or terephthalic acid were run at concentrations of 2.0×10^{-3} M and ionic strengths of $\mu = 0.10$ M (NMe_4Cl). At least 10 points per neutralization of every hydrogen ion equivalent were acquired, repeating titrations until satisfactory agreement was obtained. A minimum of three consistent sets of data was used in

(2) Bowman-James, K. *Acc. Chem. Res.* **2005**, *38*, 671−678.
(3) (a) Bradshaw, J. S. *Aza-Crown Macrocycles*; Wiley: New York, 1993. (b) Aoki, S.; Kimura, E. *Rev. Mol. Biotechnol.* **2002**, *90*, 129−155. (c) Bazzicalupi, C.; Bencini, A.; Berni, E.; Ciattini, S.; Bianchi, A.; Giorgi, C.; Paoletti, P.; Valtancoli, B. *Inorg. Chim. Acta* **2001**, *317*, 259−267. (d) Nelson, J.; Nieuwenhuyzen, M.; Pàl, I. M.; Town, R. *Chem. Commun.* **2002**, 2266−2267. (e) Dapporto, P.; Formica, M.; Fusi, V.; Micheloni, M.; Paoli, P.; Pontellini, R.; Romani, P.; Rossi, P. *Inorg. Chem.* **2000**, *39*, 2156−2163. (f) Kumar Chand, D.; Schneider, H.-J.; Aguilar, J. A.; Escart, F.; Garcia-España, E.; Luis, S. V. *Inorg. Chim. Acta* **2000**, *316*, 71−78. (g) Escarti, F.; Miranda, C.; Lamarque, L.; LaTorre, J.; Garcia-España, E.; Kumar, M.; Arán, V.; Navarro, P. *Chem. Commun.* **2002**, 936−937.
(4) García-España, E.; Díaz, P.; Llinares, J. M.; Bianchi, A. *Coord. Chem. Rev.* **2006**, *250*, 2952−2986.
(5) Nelson, D. L.; Cox, M. M. *Lehninger Principles of Biochemistry*; Worth publishers: New York, 2000.
(6) (a) Sessler, J. L.; Sansom, P. I.; Andrievsky, A.; Kral, V. Application Aspects Involving the Supramolecular Chemistry of Anions. In *Supramolecular Chemistry of Anions*; Bianchi, A., Bowman-James, K., García-España, E., Eds.; John Wiley and Sons: New York, 1997; pp 355−419. (b) Hodacová, J.; Chadim, M.; Závada, J.; Aguilar, J.; García-España, E.; Luis, S. V.; Miravet, J. F. *J. Org. Chem.* **2005**, *70* (6), 2042−2047. (c) Anda, C.; LLobet, A.; Martell, A. E.; Reibenspies, J.; Berni, E.; Solans, X. *Inorg. Chem.* **2004**, *43*, 2793−2802.
(7) Carvalho, S.; Delgado, R.; Fonseca, N.; Félix, V. *New J. Chem.* **2006**, *30*, 247−257.
(8) Anda, C.; Llobet, A.; Martell, A. E.; Donnadieu, B.; Parell, T. *Inorg. Chem.* **2003**, *42*, 8545−8550.
(9) (a) Gran, G. *Analyst (London)* **1952**, *77*, 661−663. (b) Rossotti, F. J.; Rossotti, H. *J. Chem. Educ.* **1965**, *42*, 375−378.
(10) Pettit, L. D.; Powell, K. J. *IUPAC Stability Constants Database*; Academic Software: Sourby Old Farm, Timble, Ottley, Yorks, U.K., 2004; E-mail: scdbase@acadsoft.co.uk.
(11) Smith, R. M.; Martell, A. E. *NIST Critically Selected Stability Constants: Version 2.0*; National Institute of Standards and Technology: Gaithersburg, MD, 1995.

Table 1. Logarithms of the Protonation Constants (K_i^H) for Ligand *P*3 and Substrates (S = *ph*, *is*, and *te*) at 25.0 °C and μ = 0.10 M (NMe_4Cl)[a]

equilibrium quotient (L)	*P*2	Me_6P2	*P*3 (Me_4NCl)	*P*3 (KCl)	Me_2P3 (KCl)	eq. quotient (S)	*ph*	*is*	te
K_1^H[HL]/[L][H]	9.54	8.93	10.20(2)	10.55	10.41	K_1^H[HS]/[S][H]	5.011(2)	4.42(2)	4.50
K_2^H[H_2L]/[HL][H]	8.90	8.22	10.07(2)	10.06	9.82	K_2^H[H_2S]/[HS][H]	2.738(2)	3.48(3)	3.61
K_3^H[H_3L]/[H_2L][H]	8.26	7.35	8.52(2)	8.56	8.82				
K_4^H[H_4L]/[H_3L][H]	7.50	6.44	7.62(2)	7.67	7.87				
K_5^H[H_5L]/[H_4L][H]	3.18	1.50	7.03(2)	7.12	6.79				
K_6^H[H_6L]/[H_5L][H]	3.05		6.65(2)	6.70	6.27				
$\Sigma \log K_i^H$	40.42	32.44	50.09(2)	50.66	49.98				
reference	6c	19	this work	8	7		this work	this work	11

[a] Charges have been omitted for clarity. Values in parentheses are the standard deviations in the last significant figure.

each case to calculate the overall stability constants and their standard deviations. The range of accurate p[H] measurements was considered to be 2−12. Equilibrium constants and species distribution diagrams were calculated using the program HYPERQUAD.[12]

NMR Spectroscopy. ^{1}H NMR spectra in D_2O solution at different pH values were recorded at 298 K in a Bruker 500 MHz spectrometer. The peak positions are reported relative to the residual HOD at 4.79 ppm. Small amounts of 0.01 mol·dm^{-3}·NaOD or DCl solutions were added to a solution of the ligand to adjust the pD. The pH was calculated from the measured pD values using the following relationship: pH = pD − 0.40.[13] Self-diffusion experiments were performed using the BPLED pulse sequence using a diffusion time of 150 ms and an LED delay of 5 ms. For each experiment, sine-shaped pulsed-field gradients with a duration of 1.5 ms followed by a recovery delay of 100 μs were incremented from 2% to 95% of the maximum strength in 16 equally spaced steps. Diffusion coefficients were obtained by measuring the slope in the following linear relationship: $\ln(A_g/A_o) = -\gamma^2 g^2 \delta^2 (4\Delta - \delta) D$ where A_g and A_o are the signal intensities in the presence and absence of PFG, respectively, γ is the gyromagnetic ratio (rad s g^{-1}), g is the strength of the diffusion gradients (gauss cm^{-1}), D is the diffusion coefficient of the observed spins (cm^2 s^{-1}), δ is the length of the diffusion gradient (s), and Δ is the time separation between the leading edges of the two diffusion pulsed gradients (s).

Theoretical Calculations. The molecules studied theoretically were manually built using the program MacroModel[14] and were fully minimized with the AMBER* force field.[15] A conformational analysis was done for each of the molecules to obtain the most representative conformation. A Metropolis MonteCarlo method was used, and the most stable conformation was considered.

The geometry of each molecule computed was fully optimized using Gaussian-98 program.[16] The theoretical calculation was carried out at MP2 level, and the electrostatic potential was computed using the 6-31G* basis set with the Merz−Singh−Kollman population analysis (pop = mk). The module RESP implemented in the AMBER 7 package was used to compute a final set of atomic charges for each molecule. The atomic charges were needed for the building of the molecules in AMBER.[17]

In this Study, the AMBER force field was used with a set of parameters gaff[18] implemented in the AMBER 7.0 package. Each molecule was first minimized in vacuum, and then the system was gradually heated from 1 to 298 K during 30 ps and was equilibrated for 70 ps at 298 K. This procedure was followed by another equilibration for 100 ps. The productive run was then performed in gas phase at 298 K using a time step of 1 fs and a length of 1 ns.

Results

Formation of Ternary Species H:*P*3:S. In the present Work, we describe the recognition capacities of the *P*3 hexaazamacrocyclic ligand receptor, where the amines are linked by paracyclophane spacers and by propylene groups, with regard to three aromatic dicarboxylic acids (*da*) and their anionic species (see Chart 1). Table 1 displays the protonation constants of the *P*3 ligand and also of the related *P*2, Me_6P2, and Me_2P3 for purposes of comparison. The species distribution diagram of *P*3 as a function of p[H] is presented as Figure S1 in the Supporting Information. Secondary amines are much more basic than tertiary[6c,19] (compare *P*2 and Me_6P2), but for the particular case of Me_2P3[7] and *P*3,[8] they possess relatively similar overall basicity with values of 49.98 and 50.64, respectively (see Table 1).

Potentiometric titrations were used to obtain information about the strength of the ligand−substrate interaction. With the individual protonation constants for the *P*3 ligand and substrates precisely known, the potentiometric data of a solution containing an equimolecular amount of ligand and substrate can be resolved. This gives the log K^R values of the species generated that are presented in Table 2 for *P*3 and the three dicarboxylic acids studied; furthermore, Table

(12) Gans, P.; Sabatini, A.; Vacca, A. *Talanta* **1996**, *43*, 1739−1753.
(13) Covington, A. K.; Paabo, M.; Robinson, R. A.; Bates, R. G. *Anal. Chem.* **1968**, *40*, 700.
(14) *MacroModel*, version 9.0; Schrödinger, LLC: New York, 2005.
(15) (a) Weiner, S. J.; Kollman, P. A.; Case, D. A.; Singh, U. C.; Ghio, C.; Alagona, G.; Profeta, S., Jr.; Weiner, P. *J. Am. Chem. Soc.* **1984**, *106*, 765−784. (b) Weiner, S. J.; Kollman, P. A.; Nguyen, D. T.; Case, D. A. *J. Comput. Chem.* **1986**, *7* (*2*), 230−252.
(16) Frisch, M. J.; Trucks, G. W.; Schlegel, H. B.; Scuseria, G. E.; Robb, M. A.; Cheeseman, J. R.; Zakrzewski, V. G.; Montgomery, J. A., Jr.; Stratmann, R. E.; Burant, J. C.; Dapprich, S.; Millam, J. M.; Daniels, A. D.; Kudin, K. N.; Strain, M. C.; Farkas, O.; Tomasi, J.; Barone, V.; Cossi, M.; Cammi, R.; Mennucci, B.; Pomelli, C.; Adamo, C.; Clifford, S.; Ochterski, J.; Petersson, G. A.; Ayala, P. Y.; Cui, Q.; Morokuma, K.; Salvador, P.; Dannenberg, J. J.; Malick, D. K.; Rabuck, A. D.; Raghavachari, K.; Foresman, J. B.; Cioslowski, J.; Ortiz, J. V.; Baboul, A. G.; Stefanov, B. B.; Liu, G.; Liashenko, A.; Piskorz, P.; Komaromi, I.; Gomperts, R.; Martin, R. L.; Fox, D. J.; Keith, T.; Al-Laham, M. A.; Peng, C. Y.; Nanayakkara, A.; Challacombe, M.; Gill, P. M. W.; Johnson, B.; Chen, W.; Wong, M. W.; Andres, J. L.; Gonzalez, C.; Head-Gordon, M.; Replogle, E. S.; Pople, J. A. *Gaussian 98*; Gaussian, Inc.: Pittsburgh, PA, 2001.
(17) Case, D. A.; Pearlman, D. A.; Caldwell, J. W.; Cheatham, T. E., III; Wang, J.; Ross, W. S.; Simmerling, C.; Darden, T.; Merz, K. M.; Stanton, R. V.; Cheng, A.; Vincent, J. J.; Crowley, M.; Tsui, V.; Gohlke, H.; Radmer, R.; Duan, Y.; Pitera, J.; Massova, I.; Seibel, G. L.; Singh, U. C.; Weiner, P.; Kollman, P. A. *Amber 7 User's Manual*; University of California: CA, 2002.
(18) Wang, J.; Wolf, R. M.; Caldwell, J. W.; Kollamn, P. A.; Case, D. A. *J. Comput. Chem.* **2004**, *25*, 1157−1174.
(19) Bazzicalupi, C.; Bencini, A.; Bianchi, A.; Fusi, V.; Giorgi, C.; Granchi, A.; Paoletti, P.; Valtancoli, B. *J. Chem. Soc., Perkin Trans.* **1997**, *2*, 775−781.

Table 2. Logarithms of Stepwise Association Constants (K_i^R)[a] for the Interaction of Ligand *P*3 with Substrates (S = *ph*, *is*, and *te*) at 25.0 °C and μ = 0.10 M (NMe_4Cl)[b]

stoich. L S H	equilibrium (L = *P*3)	*P*3-*is*	*P*3-*ph*	*P*3-*te*	Me_2*P*3-*is*	Me_2*P*3-*ph*
111	[HLS]/[HL][S]					
112	$[H_2LS]/[H_2L][S]$		2.75(8)			1.79
113	$[H_3LS]/[H_3L][S]$	3.07(8)	2.79(6)	2.58(9)		2.42
114	$[H_4LS]/[H_4L][S]$	3.96(5)	2.85(6)	2.80(1)	2.41	2.67
115	$[H_5LS]/[H_5L][S]$	3.73(2)	3.47(5)	2.83(2)	2.68	3.05
116	$[H_6LS]/[H_6L][S]$	4.74(5)	3.70(3)	3.45(1)	3.02	3.38
117	$[H_7LS]/[H_6L][HS]$	4.29(7)	2.14(7)		2.72	2.69
118	$[H_8LS]/[H_6L][H_2S]$	4.11(7)				
	reference	this Work	this Work	this Work	7	7

[a] Log K_i^R are calculated by subtraction of the logs of the cumulative protonation constants of the individual ligands and substrates (Table S1; Log β_{HiL}, Log β_{HiS}) from the logs of the cumulative formation constants reported in Table S2 (Log β_{HiLS}). As an example, Log K_8^R is calculated using the following equation: $\text{Log}[K_8^R] = \text{Log}[\beta_{H8LS}] - \text{Log}[\beta_{H6L}] - \text{Log}[\beta_{H2S}]$. [b] Charges have been omitted for clarity. Values in parentheses are the standard deviations in the last significant figure.

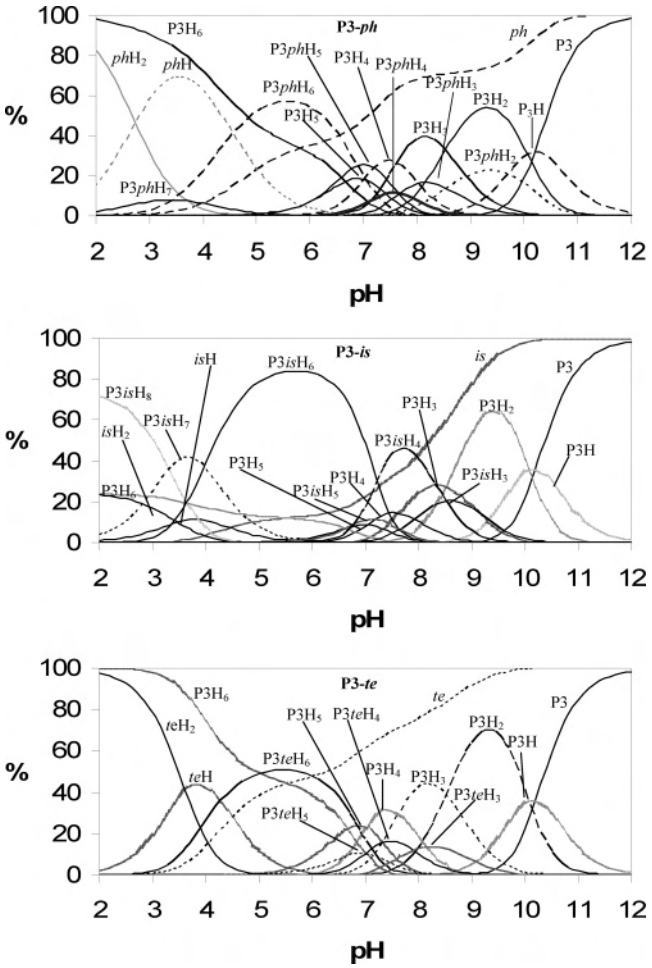

Figure 1. Species distribution diagram as a function of p[H] for the *P*3-*ph*, *P*3-*is*, and *P*3-*te* systems.

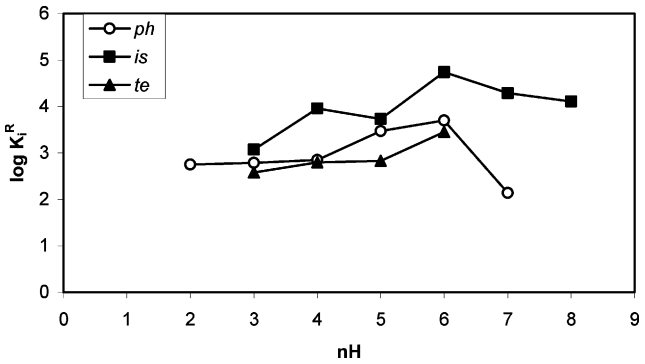

Figure 2. Log K_i^R versus *n*H (the different ternary species with various degrees of protonation) for the three systems *P*3-S.

2 also contains the log K^R values of related systems for purposes of comparison. For the *P*3-*is* system, the presence of six equilibrium species is detected and can be expressed as shown in Table 2, where K_i^R is the recognition constant of protonation degree *i* and is listed in order of appearance from high to low p[H].

Figure 1 displays the species distribution diagrams as a function of p[H] obtained for the three systems *P*3-*is*, *P*3-*ph*, and *P*3-*te*. For the *P*3-*is* system, it is interesting to note that over the p[H] range 2−8 the predominant species is H_i:*P*3:*is* rather than the individual species derived from protonation of the ligand and substrates (this range is reduced to 5−6.8 and 5−6.2 for the *P*3-*ph* and *P*3-*te* systems, respectively). The highest equilibrium constant corresponds to the formation of the species H_6P3is^{4+}, log K_6^R = 4.74, where Coulombic interaction and potential hydrogen bonding reach a maximum. This species is largely predominant over the p[H] range 4−7 as can be observed in Figure 1. Table 2 also displays the recognition constants for the other carboxylic acids studied that are lower than for the case of *P*3-*is* system; this is also graphically shown in Figure 2 where log K_i^R is plotted against *n*H, the degree of protonation of the ternary species. Table 2 also shows the recognition constants of the same substrates but using the Me_2P3 ligand for purposes of comparison; those constants are in general lower than for the corresponding *P*3 ligand and also are within the range of host−guest interactions with cyclic and acyclic receptors and carboxylic acids reported in the literature.[20]

(20) (a) Hosseini, M. W.; Lehn, J.-M. *J. Am. Chem. Soc*. **1982**, *104*, 3525−3527. (b) Hosseini, M. W.; Lehn, J.-M. *Helv. Chim. Acta* **1986**, *69*, 587. (c) Lehn, J.-M.; Meric, R.; Vigneron, J.-P.; Waksman-Bkouche, I.; Pascard, C. *J. Chem. Soc., Chem. Commun*. **1991**, 62−64. (d) Dietrich, B.; Hosseini, M. W.; Lehn, J.-M.; Sessions, R. B. *J. Am. Chem. Soc*. **1981**, *103*, 1282−1283. (e) Kimura, E.; Sakonaka, A.; Yatsunami, T.; Kodama, M. *J. Am. Chem. Soc*. **1981**, *103*, 3041−3049. (f) Bencini, A.; Bianchi, A.; Burguete, M. I.; García-España, E.; Luis, S. V.; Ramírez, J. A. *J. Am. Chem. Soc*. **1992**, *114*, 1919−1921. (g) Lu, Q.; Motekaitis, R. J.; Reibenspies, J. J.; Martell, A. E. *Inorg. Chem*. **1995**, *34*, 4958. (h) Motekaitis, R. J.; Martell, A. E. *Inorg. Chem*. **1996**, *35*, 4597.

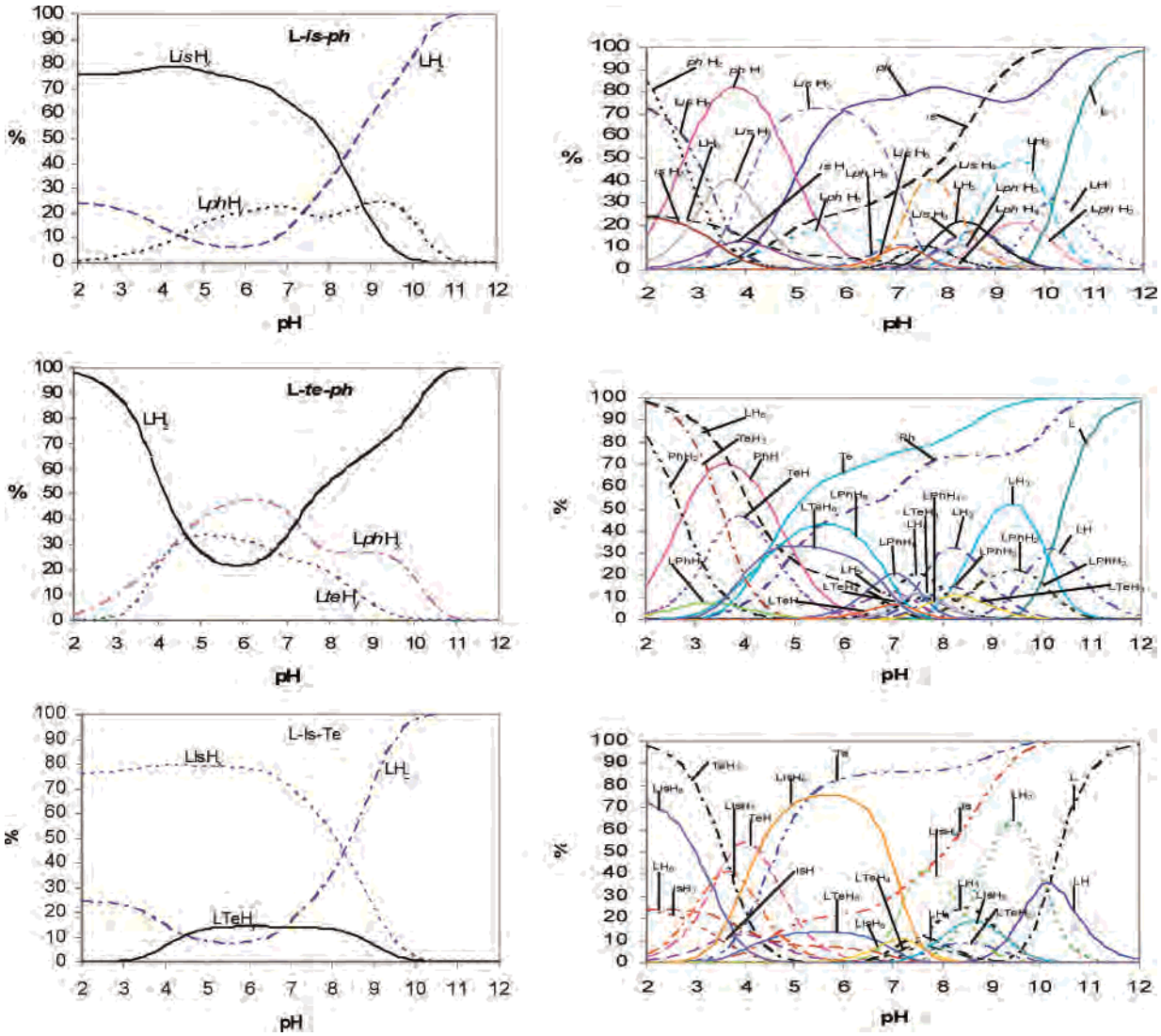

Figure 3. Competitive calculated species distribution diagram and total species distribution diagrams for systems with equimolecular amounts of L-S (*P*3, *ph*, *is*, *te*).

Interaction Site and Selectivity. Figure 2 shows a graphical representation of the different recognition constants as a function of proton content obtained for the *P*3 systems formed with three diacidic substrates. From the graph, it is clear that the log K_i^R and thus the bonding strength follow the sequence *P*3-*is* > *P*3-*ph* > *P*3-*te* clearly manifesting the importance of the geometrical fit between substrate and receptor. This is further illustrated in Figure 3 where for the *P*3-*is*-*te* competitive system, the *P*3:*is*:H_i species always predominates over the *P*3:*te*:H_i species. At pH 5.0 for instance, the selectivity of *is* containing species over *te* is 89%; the selectivity for *is* containing species over *te* at a particular pH is defined according to the following equation:

$$\left\{\sum_i (\%P3{:}is{:}H_i)/[\sum_i (\%P3{:}is{:}H_i) + \sum_i (\%P3{:}te{:}H_i)]\right\} \times 100$$

^{1}H NMR spectroscopy was also used to characterize the complexation process and to identify the site of interaction between the *P*3 macrocycle and three aromatic dicarboxylic derivatives, namely, *is*, *ph*, and *te* in binary complexes. NMR spectra were recorded at pH = 5.5 because of large abundance of the H_6*P*3*is* species. Table 3 summarizes the most important NMR related features including CISs (complexation induced shifts), intermolecular nuclear Overhauser effects (NOEs), and self-diffusion coefficients (*D*) of the studied complex, whereas a full set of key NMR spectra are displayed as Supporting Information. CIS and *D* values confirm the existence of host−guest complexation, whereas the intermolecular host−guest NOEs allow us to get more insight about the geometry and the main contact points between the different diacid compounds and the macrocyle.

It can be shown that an equimolecular mixture of *P*3 and *da* produces a general CIS effect that mostly affects the aromatic protons of both diacid and cyclophane derivatives because of the anisotropic features of the aromatic rings (Table 3). Furthermore, the aliphatic chain of *P*3 is also slightly affected by the complexation process specially the CH_2 benzylic protons labeled as $(CH_2)_d$ in Chart 1. In the case of the *P*3-*is* system, the major CIS effect is observed for the H_h proton, and strong intermolecular NOEs are observed between α-N−CH_2^b and α-N−CH_2^c of *P*3 and all the aromatic protons of *is*, putting forward the most important

Table 3. NMR Data of 1:1 2 mM Binary *da*-*P*3 Complexes

			$D \times 10^{-10}$ cm^2/s	
	CIS[a]	NOEs[b]	D(*P*3)[c]	D(*da*)[d]
*P*3:*is*	H_h: 8.28−8.06	$(CH_2)^{b,c}$ - ar-*is* (s)	3.0 ± 0.2	4.3 ± 0.2
	H_i: 7.98−7.91	$(CH_2)^{a,d}$ - ar-*is* (m)		
	H_j: 7.52−7.47	ar-*P*3 - ar-*is* (w)		
	Ar: 7.56−7.45			
	CH_2^a: 2.05−2.00			
	CH_2^b: 3.06−3.00			
	CH_2^c: 3.06−3.00			
	CH_2^d: 4.31−4.19			
*P*3:*ph*	H_h: 7.47−7.32	$(CH_2)^{b,c}$ - ar- *ph* (s)	3.0 ± 0.2	3.8 ± 0.2
	H_i: 7.41−7.23	$(CH_2)^{a,d}$ - ar-*ph* (m)		
	Ar: 7.56−7.44	ar-*P*3 - ar-*ph* (w)		
	CH_2^a: 2.05−1.92			
	CH_2^b: 3.06−2.92			
	CH_2^c: 3.06−2.88			
	CH_2^d: 4.31−4.17			
*P*3:*te*	H_i: 7.88−7.63	$(CH_2)^{b,c}$ - ar-*te* (s)	3.0 ± 0.2	3.9 ± 0.2
	Ar: 7.56−7.51	$(CH_2)^{a,d}$ - ar-*te* (m)		
	CH_2^a: 2.05−1.97	ar-*P*3 - ar-*te* (w)		
	CH_2^b: 3.06−3.01			
	CH_2^c: 3.06−2.91			
	CH_2^d: 4.31−4.23			

[a] Experimental chemical shift changes in ppm upon complexation in a ratio 1:1. [b] s: strong, m: medium, w: weak. [c] The D value of the free *P*3 ligand is 3.1 ± 0.2 × 10^{-10} m^2/s. [d] The D values of the free substrates are 5.2 ± 0.2 × 10^{-10} m^2/s for *is*, 5.2 ± 0.2 × 10^{-10} m^2/s for *ph*, and 5.1 ± 0.2 × 10^{-10} m^2/s for *te*.

contact points in the receptor−substrate complex. Very importantly, only weak NOEs can be detected between the aromatic *is* protons and the N−CH_2^a and N−CH_2^d menthylenic protons and between the aromatic protons of *P*3 and *is*, indicating that π-stacking interactions are not predominant in this system. Relatively similar behaviors are also observed for the other two diacid systems and thus will not be further described here.

The formation of the complex is evident from the large variation of the experimental diffusion coefficient obtained for the small dicarboxylic acid molecule, D(*da*), as a function of its concentration whereas D of the macrocycle, D(*P*3), remains practically unaltered (Table 3).[21] The large chemical shift deviations and the similar D values observed for both *P*3 and *is* resonances in high [*P*3]:[*is*] ratio confirms that the acid is strongly attached into the cationic ligand receptor. When [*is*] increases, dynamic processes combining several possible free and complexed geometries are active where the guest is in fast equilibrium between the outside and the inside of the macrocyclic cavity (see Table 4).

Theoretical Calculations. Theoretical calculations were performed at MP2 level using the 6-31G* set of basis to get further insight into the site of interaction between receptor and substrate. Those calculations also allow visualizing the complexed structures and a quantitative evaluation of their bonding strength. Figure 4 displays two views (left, stick; right, compact) of the average calculated structure for the three systems studied in the present work. An overlaying of the 25 most significant structures is presented as Supporting Information. Table 5 displays the energies obtained for the free ligand and substrates and also of the complexed species. From Figure 4, it can be observed that the *P*3 ligand interacts

(21) Fielding, L. *Tetrahedron* **2000**, *56*, 6151.

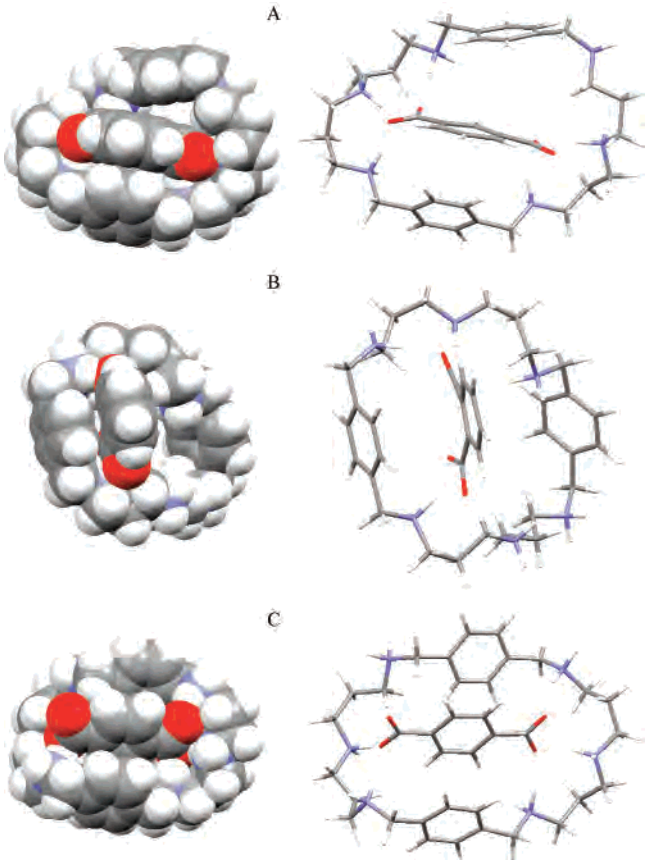

Figure 4. van der Waals space filling (left) and stick (right) views of average calculated structures studied by molecular dynamics in vacuum for (A) *P*3-*is*, (B) *P*3-*ph*, and (C) *P*3-*te* systems.

Table 4. Measured Self-Diffusion Coefficients for *P*3 and *is* in Free and Complex States

[*P*3]:[*is*]	D(*P*3) × 10^{-10} cm^2/s	D(*is*) × 10^{-10} cm^2/s
1:0	3.1 ± 0.2	
0:1		5.2 ± 0.2
1:0.1	3.1 ± 0.2	3.2 ± 0.2
1:0.5	3.0 ± 0.2	4.0 ± 0.2
1:1	3.0 ± 0.2	4.3 ± 0.2
1:1.5	3.2 ± 0.2	4.6 ± 0.2
1:2	3.1 ± 0.2	4.8 ± 0.2

Table 5. Total Energies and Complexation Energies for the Anionic Complexes *P*3-*da*

	E_{tot} (kcal/mol)	StD[a]	E_c (kcal/mol)
is^{2-}	−194.2528	0.2348	
ph^{2-}	−193.1369	0.2880	
te^{2-}	−177.7070	0.1807	
$H_6P_3^{6+}$	−671.0568	16.6535	
$is^{2-} + H_6P_3^{6+}$	−939.4684	25.9589	−74.1588
$ph^{2-} + H_6P_3^{6+}$	−923.3875	24.9323	−59.1938
$te^{2-} + H_6P_3^{6+}$	−894.6212	38.3180	−45.8574

[a] Standard deviation.

with substrate *is* through four strong H-bonds whereas substrate *ph* interacts through three and *te* only through two. This number of strong H-bonds for each complex species correlates with the obtained complexation energies displayed in Table 5 where the energy released upon complexation follows the order meta (*P*3-*is*) > orto (*P*3-*ph*) > para (*P*3-*te*). The zone of interaction between the *P*3 receptor and the

ligand substrates is in agreement with the structural description acquired by the NMR experiments described in the previous section.

Discussion

The basicity of a given ligand receptor usually plays a key role[1j,6c,8,22] with regard to its anionic bonding capacities together with its size, shape, and flexibility. The ligands Me_2P3 (two tertiary amines + four secondary amines) and *P*3 (six secondary amines) have very similar overall protonation constants. The fact that the first four protonation constants differ in only 0.14−0.26 log units indicates that the main protonation sites in both cases are the secondary amines. For the fifth and sixth protonation constants, the differences now increase only up to 0.33−0.43 log units. These small differences clearly manifest that in this particular case charge separation becomes a dominant factor over the secondary versus tertiary amine effects.

Potentiometric titrations and NMR spectroscopy unambiguously reveal the formation of anionic complexes between dicarboxylic acids (*da*) and the *P*3 ligand receptor (Tables 2 and 3) as had also been previously shown for the Me_2P3 case[7] (see Table 2). In sharp contrast, however, for the latter the ligand interacts with the *da* substrates with comparable strength, and for the former there is a large difference between the recognition capacity for the three different *da* substrates. As an example, the recognition capacity of the *P*3 ligand receptor over the *da* substrate is exemplified by a selectivity of over 89% at p[H] = 5.0 in favor of the *is* substrate versus the *te*. Furthermore, whereas the largest recognition constant log K_6^R is 3.02 for Me_2P3 and *is*, for *P*3 it increases by more than 1.7 orders of magnitude to a value of 4.74.

Given the close similarities in the basicity and size of the two ligands, the discriminatory effect can only be attributed to the more restricted rotation of tertiary versus secondary central amines with the conformational consequences that this implies. In addition, the relative capacity of these central amines to form H-bonds with the substrates will also be responsible for the discriminating phenomenon. In this sense and as shown in Figure 4, the *P*3 central amines are involved in the formation of H-bondings with all three substrates. For the *ph* and *is* substrates, the H-bonding is further extended to the benzylic amines thus providing multiple H-bonding sites whose strength depends on the geometry of the substrate and the capacity of the *P*3 ligand to adapt to the substrate geometry. This results in four strong H-bonds with *is*, three with *ph*, and two with *te* which also correlates with the calculated complexation energies (see Table 5) as mentioned in the previous section.

In conclusion, the replacement of tertiary central amines in Me_2P3 by secondary amines in *P*3 produces a new conformational scenario that together with their stronger capacity to form H-bonds with the dicarboxylic acid substrates is responsible for the spectacular change in selectivity of the mentioned ligand receptors versus the substrates. This Work constitutes an example of how subtle ligand variations cause dramatic recognition capacities and thus is useful for the design of future ligand receptors.

Acknowledgment. This research has been financed by MEC of Spain through projects CSD2006-003, CTQ2007-67918, CTQ2006-01080, CTQ2006-08256 and also partially, using CESCA resources. A. A. is grateful for the award of a doctoral grant from CIRIT Generalitat de Catalunya.

Supporting Information Available: Additional, structural, and spectroscopic (NMR) data. This material is available free of charge via the Internet at http://pubs.acs.org.

IC701288N

(22) Bazzicalupi, C.; Bencini, A.; Bianchi, A.; Borsari, L.; Giorgi, C.; Valtancoli, B. *J. Org. Chem.* **2005**, *70* (11), 4257−4266.